CULHAM LIBRARY
REFERENCE ONLY

CULHAM LABORATORY
LIBRARY
- 4 MAY 1976
b.

UKAEA RESEARCH GROUP

Report

# STRUCTURAL DESIGN OF DEMOUNTABLE BLANKET ELEMENTS AND SHIELD FOR A FUSION REACTOR

H M CARRUTHERS

CULHAM LABORATORY
Abingdon Oxfordshire
1976

Available from H. M. Stationery Office

C18

£1.00

Enquiries about copyright and reproduction should be addressed to the Librarian, UKAEA, Culham Laboratory, Abingdon, Oxon. OX14 3DB, England.

UDC 621.039.63

CLM-R 151

# STRUCTURAL DESIGN OF DEMOUNTABLE BLANKET ELEMENTS AND SHIELD FOR A FUSION REACTOR

by

H.M. Carruthers

Associated Nuclear Services, Epsom, UK

## ABSTRACT

Tentative design ideas are presented for a lithium-cooled blanket consisting of sub-assemblies each of about 25 cylindrical cells. A possible form of magnet shield, which also serves as the vacuum vessel of the reactor and the structure from which the blanket is supported, is described. Major problems, some of them linked with the toroidal geometry and others specific to the use of lithium coolant, are discussed.

This work was carried out by Associated Nuclear Services for Culham Laboratory under Contract No. MIA 67398.

Culham Laboratory
Euratom/UKAEA Fusion Association
Abingdon
Oxon

September 1975

SBN 85311 039 5

## CONTENTS

SYMBOLS

1. INTRODUCTION

2. PRELIMINARY DESIGN CONSIDERATIONS
   - 2.1 Location of vacuum boundary
   - 2.2 Rejection of the blanket/shield element concept

3. SHIELD DESIGN
   - 3.1 General arrangement
   - 3.2 Shield cooling

4. BLANKET SUB-ASSEMBLY DESIGN
   - 4.1 Main design options
   - 4.2 Sub-assembly design pressure
   - 4.3 General arrangement of typical sub-assembly

5. ARRANGEMENT OF CELL SUB-ASSEMBLIES INSIDE SHIELD
   - 5.1 Outer vertical panels
   - 5.2 Lower inclined panels
   - 5.3 Roof panels
   - 5.4 Inner vertical panels
   - 5.5 Handling of blanket sub-assemblies

6. DISCUSSION

7. ACKNOWLEDGEMENTS

8. REFERENCES

APPENDIX A Stress calculations on shield structure

APPENDIX B Shield cooling requirements

APPENDIX C Problems arising from heat conduction and radiation within the blanket sub-assembly and shield

APPENDIX D Design pressure for outlet header

APPENDIX E Thermal stresses within the blanket structure and support

APPENDIX F Stresses in thermal sleeves due to dead load

## SYMBOLS

| | |
|---|---|
| $a$ | pipe radius |
| $A$ | cross sectional area of flow |
| $b$ | breadth of shield panel |
| $B$ | magnetic flux density |
| $E$ | Young's Modulus |
| $I$ | second moment of area |
| $q$ | radiant heat loss per unit area |
| $r$ | minor radius of torus |
| $R$ | major radius of torus |
| $t$ | pipe wall thickness |
| $W$ | mass flow |
| $\alpha$ | coefficient of thermal expansion |
| $\delta$ | deflection |
| $\rho$ | density |
| $\sigma$ | stress |
| $\sigma_w$ | electrical conductivity of pipe wall |

# STRUCTURAL DESIGN OF DEMOUNTABLE BLANKET ELEMENTS AND SHIELD FOR A FUSION REACTOR

by

H.M. Carruthers

## 1. INTRODUCTION

Development work on the structural design of the blanket and shield for a 5 GW (t) Tokamak fusion reactor is described in this report. Associated studies in connection with irradiation creep, swelling, and helium embrittlement of the blanket cell material are reported separately, (Ref. 1).

The relevant reactor parameters and design features which were adopted as the starting point for the study are listed in Table 1.

| | |
|---|---|
| **Reactor** | |
| Thermal wall loading | MW/m$^2$ 1.31 |
| Heat per unit blanket area | MW/m$^2$ 1.191 |
| Major radius | m 16.7 |
| Minor radius | m 5.8 |
| **Blanket** | |
| Type | cellular (cylindrical cells) |
| Coolant | lithium |
| Cell diameter | m 0.3 nominal |
| Cell length | m 0.6 " |
| Material of cells, coolant headers and pipework | stainless steel Type 304 |
| **Magnet Shield** | |
| Materials (see Appendix A, Fig. A1) | stainless steel Type 304<br>borated water<br>lead |
| **Magnet Coils** | |
| Leading dimensions of "D"-shape: | |
| Internal height | m ~ 29 |
| Internal width | m ~ 17 |
| Radial thickness of conductors | m 1.0 |
| Max.toroidal flux density | tesla 8.0 |

Table 1. Leading reactor parameters and design features used as basis of study

On the basis of earlier conceptual design work carried out at Culham, (Ref. 2), it was decided to develop a concept in which the blanket elements or sub-assemblies are mounted in and removable from a shield structure which is only demountable to the extent necessary to gain access to the blanket. It was further decided that the design work would deal only with the lithium-cooled version, rather than attempting also to cover the alternative of helium coolant.

As will be seen from the following sections of this report, it has only been possible in the time available to develop one design concept to a stage at which some of the more severe problems, particularly in regard to differential thermal expansion, are either eliminated or mitigated. Much more detailed work would be required before the viability of a blanket and shield design based on the concept described could be confirmed. It is recognised that such work would almost certainly lead to many changes of detail, and quite possibly to the abandonment of one or more of the main features in the suggested arrangement.

## 2. PRELIMINARY DESIGN CONSIDERATIONS

### 2.1 Location of vacuum boundary

At the outset of the study consideration was given to the location of the boundary within which the high vacuum necessary for the plasma would be maintained. This was necessary because of the possible influence of the vacuum wall on the design of either the blanket structure or the shield. Against the background of earlier work on this question, (Ref. 2), the following locations were considered;

(a) between the blanket and the shield,

(b) on the outer surface of the shield, or

(c) between the shield and the magnet coils.

A free-standing vacuum vessel in position (a) or (c) would have to be a massive structure in order to achieve stability against the external overpressure, and it would therefore occupy valuable space, increasing the dimensions of the shield and magnet coils if at (a) or the magnet coils if at (c). Location at (a) would also give rise to problems of achieving vacuum-tight seals at the many inaccessible penetrations for coolant pipes, and would present additional problems connected with the removal of heat generated by gamma and neutron irradiation of the vacuum wall.

It was therefore decided to design the shield to withstand loads due to its own weight, the weight of the blanket, and atmospheric pressure on its outer surface. It appeared likely that the thickness of the shield dictated by gamma and neutron flux attenuation requirements would be adequate to enable the shield structure to fulfil the vacuum load requirement with little or no extra expenditure of material, and the stress calculations carried out later in the exercise confirm that this is so.

### 2.2 Rejection of the blanket/shield element concept

Judging from earlier work, e.g. Ref. 3, material damage of the inner surface of the shield would not necessitate periodic replacement of the structure, and this fact, together with the reasoning presented in Ref. 2, led to the shield being envisaged as a substantially permanent structure with the minimum number of mechanical joints, all of which would be made vacuum tight by seal welding. The only moveable sections of shield would be those which would have to be displaced in order to gain access to the blanket. The blanket cells would be grouped in sub-assemblies mounted on the inner surface of the shield.

The resulting design concept was then elaborated to the extent indicated in the following sections.

## 3. SHIELD DESIGN

### 3.1 General arrangement

For stress calculation purposes it was assumed that the shield would comprise 96 sectors, each subtending an angle of 3.75° at the centre-line of the torus. The vertical cross section of each sector would be of hexagonal form as indicated in some earlier notional sketches (Ref. 4). A shield of this general form would be cheaper to fabricate than one of circular cross section, and would also require a smaller number of geometrical variations for the different blanket sub-assemblies. It appeared later in the study that an octagonal section may be preferable from the point of view of handling blanket sub-assemblies, and such a design was in fact taken for illustrative purposes in considering blanket handling and lithium pipe routing - see Section 5.3 and Figure 4. From the design and fabrication viewpoints a shield of this type would be substantially similar to the hexagonal section shield discussed in this section.

For each sector a box structure was adopted, in which the bulk of the resistance to bending moments imposed by dead loads and external pressure is provided by the plates forming the inner and outer shield surfaces. The steel and water filling of the hollow section was taken to be as proposed in Ref. 5, all internal shielding steel being considered as dead weight.

The vertical sides and the two bottom panels of each sector of the shield are welded into a structure in the form of a ⋃ - section trough. The top two panels of each sector are a separate roof fabrication which is normally seal-welded to the trough and to its neighbouring roof sectors. This general arrangement is illustrated in Figure 1, which also shows the positions of the supporting legs.

The torus first wall aspect ratio (major radius: minor radius) assumed for this study ($\sim 3:1$) is such that the centroid of a shield sector lies $\sim 1.8$ m outside the vertical centre line of its radial cross-section, and it will be seen that the support legs have been positioned approximately under the centroid.

This eliminates stresses in the direction of the major circumference of the torus due to dead loads and correspondlingly simplifies the stress calculations, which have been restricted for the present purpose to estimations of the bending stresses in the inner and outer plates of a sector, regarded as a structure separate from the neighbouring sectors. These calculations are reproduced in Appendix A.

The complete shield structure will have a temperature range of the order of 50°C between the shutdown and operating conditions, and therefore the free radial expansion at the radius of the support legs will be approximately 20 mm. This implies that some form of roller support may be necessary, and the proposed design incorporates 24 support legs each resting on a roller of about 2 m diameter. Thus each support leg fits between two adjacent magnet coils, and supports four shield sectors.

A 1:50 scale model of the proposed design was built, showing the general appearance of six sectors of shield and their spatial relationship to the adjacent magnet coils. The main purpose of the model was to assist in the conceptual design development of the blanket sub-assemblies and the external coolant pipework. A photograph of the model is reproduced in Figure 2.

### 3.2 Shield cooling

Appendix B gives estimates of the heat generation rate in each panel of a hexagonal shield sector. It is seen that each sector of the trough part of the shield produces about 220 kW, and each sector of the roof part about 110 kW. The cooling water flow rates required per sector are modest, and this suggests that several sectors of the trough could be combined for cooling water flow purposes. Provided that the flow pattern is arranged in such a way as to avoid adjacent parts of the shield being in contact with water at inlet and outlet temperatures, no significant thermal stresses should be induced, at least in the steady state, and no further attention has been devoted to this aspect of the design.

## 4. BLANKET SUB-ASSEMBLY DESIGN

### 4.1 Main design options

The type of blanket cell which had been the subject of an earlier study (Ref. 3), was adopted for the present design development work. Two basic design options in regard to structural support of the cells were first considered. These were:

(a) to mount a group of cells on a frame whose functions would be to maintain the cell spacing and to attach the sub-assembly to the shield wall, or

(b) to mount a group of cells on a hollow structure which would combine the duties of structural support and outlet lithium header. This is the concept first proposed in Ref. 3.

Consideration of alternative (a) suggested that for a sub-assembly of say 20 or 30 cells there might be difficulty in accommodating all the individual inlet and outlet lithium pipes, bearing in mind that sufficient flexibility would have to be incorporated to cater for differential thermal expansion, and that it would be desirable to achieve this without the use of bellows. Furthermore, there would be poor thermal contact between the frame and the shield, and therefore thermal radiation would probably play a significant part in disposing of the heat generated in the frame. A simple assessment of this problem is made in Appendix C, where it is shown that since only the outward-facing surfaces towards the back of the frame would "see" the cold shield rather than the hot pipework or cells, there would be thermal stress and distortion problems due to the temperature gradients within the frame.

Therefore option (b), which inherently provides cooling for the cell support structure, was adopted for the study, despite its superficially greater complexity.

### 4.2 Sub-assembly design pressure

The pressure drop due to MHD effects in the lithium as it flows from the cell sub-assembly to the region outside the magnet coils has an important influence on the choice of design pressure for the sub-assembly. For a given number of cells, this pressure drop is a function of the outlet pipe diameter and wall thickness, the transverse magnetic flux, and the path length.

Shielding and mechanical flexibility requirements provide an incentive to limit the lithium pipe diameters as they pass through the shield, but in the relatively long runs between the shield and the magnet coils the MHD-induced pressure drop effects in the lithium will be an important consideration tending to lead to the adoption of larger diameters in order to reduce flow velocities. Appendix D discusses these aspects and presents pressure drop calculations for an outlet pipe of 215 mm diameter through the shield and 300 mm diameter downstream of the shield outer surface. For each part of the pipe a wall-thickness/pipe radius ratio of 0.014 has been assumed. The calculations indicate an absolute pressure of $\sim 0.5$ MN/m$^2$ in the outlet header. On this basis the hoop membrane stress in the first part of the oultet pipe would be given by $p\frac{a}{t} = \frac{0.5}{0.014} = 35.8$ MN/m$^2$, which is well within the permissible limits for austenitic steels at 500°C (Ref. 6).

It was decided in the light of the above reasoning to adopt a design pressure of 0.5 MN/m$^2$ in the outlet header.

### 4.3 General arrangement of typical sub-assembly

In order to enable the feasibility of the chosen type of construction to be assessed, attention was focussed on the problems of designing a sub-assembly of 25 cells of 300 mm diameter arranged on a triangular lattice in three rows of 8, 9 and 8. This would have overall dimensions of approximately 2.7 m x 0.825 m x $L_R$, where $L_R$ is the total depth in the radial direction, and therefore appeared to be a reasonable unit to handle through the limited aperture available in the shield.

The results of the design work on this typical sub-assembly are illustrated in Figure 3 and discussed below.

#### 4.3.1 Connections of inlet and outlet lithium pipes

The feasibility of remotely connecting and sealing coolant pipe joints inside the shield, with virtually 100% reliability, was considered so doubtful that it was decided to investigate the alternative of bringing the pipework through to the outside of the shield where pipe and penetration welds could be made and inspected much more readily. In order to avoid an unacceptably large number of penetrations, a single outlet pipe was adopted.

Twin inlet pipes feed lithium into a narrow box-shaped inlet header located on the back surface of the outlet header by studs in slotted holes to allow relative expansion.

#### 4.3.2 Thermal sleeves

In view of the large temperature differences between inlet and outlet pipes respectively and the shield structure to which they must be attached and hermetically sealed, thermal sleeves are provided, extending from the pipes near the inner shield surface to the shield near its outer surface. A smooth temperature gradient along the sleeves, which may call for the insertion of some metallic foil insulation in the annular spaces between them, the coolant pipes, and the shield penetration pipes, (see Appendix C, Section C2), is necessary in order to limit thermal stresses and to maintain the mechanical joints at the outboard ends at reasonably low temperatures.

The penetrations, thermal sleeves, and lithium pipes are shown on the drawing as having steps to attenuate radiation streaming, though the need for these has not been studied. Another shielding aspect which would need considering is the necessity or otherwise of some iron labyrinth in the pipes for the same purpose.

#### 4.3.3 Structural support of sub-assembly

Three-point support of the complete sub-assembly is provided by clamping the thermal sleeves of the inlet and outlet pipes against chamfered lands near the outer ends of the shield penetrations.

A notional clamping arrangement is indicated on the drawing. This consists of a split wedge-section ring pressed radially into a tapered groove in the thermal sleeve by a loose flange bolted on to the outer surface of the shield.

With this type of support, a sub-assembly in the region of the equatorial plane of the torus would be cantilevered inwards from the outer surface of the shield where its inlet and outlet sleeves are attached. A rough assessment of the stresses in the sleeves and the deflections due to the dead weight of a sub-assembly is made in Appendix F, which indicates that adequate strength and rigidity would be achieved with sleeves 10 mm thick.

It appears from Appendix E however that such single sleeves would be too rigid to accommodate thermal expansion of the inlet header, and that it may be necessary to make the inlet sleeves more flexible, e.g. by using a re-entrant design. This solution would throw more dead-load carrying duty on to the outlet sleeve, but from Appendix F it can be deduced that this should not cause any difficulty.

### 4.3.4 Outlet header design

The outlet header is basically a flat vessel, the front and back plates of which are penetrated by holes on a triangular pitch which is equal to the blanket cell diameter plus a small clearance allowance, in order to accommodate the blanket cells and lithium pipes respectively. The plates are tied together by stays arranged on a hexagonal lattice in the interstitial positions between cell centrelines. The stays are welded into both plates.

Provided that the headers are arranged with their length parallel to the direction of the magnetic flux, i.e. horizontally, the flow velocity can be relatively high without incurring much pressure drop penalty, and therefore with such an orientation the depth of the header can be quite small. For illustrative purposes, the depth of header shown on the drawing (Fig. 3) is 75 mm. This would correspond to a lithium flow velocity not exceeding twice the velocity in the outlet pipe, and a pressure drop along the header which would be negligible in comparison with that in the outlet pipe which traverses the magnetic field.

The appropriate ASME Code (Ref. 6) was used as the basis of indicative calculations of the required thickness of plates and diameter of stays for such a header. For a design pressure of 75 $lb/in^2$ ($\sim 0.5$ $MN/m^2$) and the allowable stress given by the Code for the appropriate temperature, a plate thickness of 18 mm and a stay diameter of 20 mm were indicated. However, much more detailed study would be required, taking account of edge effects, and particularly of the geometical irregularity in the region of the outlet pipe, before the design could be regarded as established.

The transition between the back plate of the header and the outlet pipe is unavoidably of unfavourable geometry from the pressure vessel viewpoint, merging from an oblong opening in the back plate, the width of the opening being limited to about 100 mm by the clearance between rows of penetrations, to the full pipe diameter. It is conceivable that this transition piece and those for the inlet header could be welded fabrications, but an alternative might be to cast them. The degree of offset shown on the drawing is arbitrary, and indeed it is possible that simpler symmetical transition pieces for both inlet and outlet pipes could be designed.

### 4.3.5 Attachment of cells and inlet pipes

It is envisaged that the necks of the bottle-shaped cells would be expanded into the holes in the front plate of the outlet header and seal welded using a suitable preparation. The same process would be used for sealing the outer members of the inlet pipes to the back plate. Established practice in forming $D_2O$-tight joints between CANDU and SGHW reactor pressure tubes and their end fittings provides evidence that this type of rolled joint may be adequate for the purpose, even without seal welding, provided that the operation is carried out under precisely controlled conditions.

### 4.3.6 Design of inlet pipes

The re-entrant pipes shown on the drawing serve the dual purpose of providing electrical and thermal insulation between in-flowing and out-flowing lithium, and providing some flexibility in the pipework system. A preliminary examination of the bending of the pipe as a result of differential thermal expansion of the inlet and outlet parts of the assembly (Appendix E) suggests that this type of construction would accommodate the movements without overstressing the pipework, and it therefore seems that bellows need not be used.

### 4.3.7 Assembly procedure

The sequence of operations necessary to build the blanket sub-assembly is illustrated in Fig. 5 and summarised below:

(1) The stays are welded into the front plate of the outlet header.

(2) The cells, at this stage without their dished ends, are expanded and welded into the front plate.

(3) The side-walls of the outlet header are welded to the back plate.

(4) The outer members of the inlet pipes are expanded and welded into the back plate.

(5) The front plate is welded to the side-walls and the stays to the back plate.

(6) The inner members of the inlet pipes are welded to the outer members at the bell-mouth, and the flow control feature is fitted.

(7) The dished ends are welded on to the cells.

(8) The inlet header is secured to the outlet header, and the inlet pipes sprung into the weld-prepared holes and welded.

## 5. ARRANGEMENT OF CELL SUB-ASSEMBLIES INSIDE SHIELD

### 5.1 Outer vertical panels

In order to enable sub-assemblies to be arranged in a close-packed array of identical units covering the rectangular area of a group of say four panels (a 15° sector) it would be necessary to delete the end cell from one end of the central row on each sub-assembly, or to add a cell to one end of each outer row, giving it either a chevron or parallelogram form rather than the elongated hexagonal shape of the unit discussed above, but this would not affect the design considerations already discussed. The area to be covered would be approximately 6.25 m wide x 8 m high, and it is suggested that two columns of eight sub-assemblies, based on a cell diameter of about 350 mm, would be a suitable basis on which to develop the design concept.

### 5.2 Lower inclined panels

A similar arrangement might be appropriate for these parts of the blanket, but the trapezoidal shape would necessitate some variation in either the number or the diameter of the cells in the different sub-assemblies. The question of whether the coolant pipe penetrations should be vertical or perpendicular to the shield surface has not been considered in detail, but from the cell sub-assembly design viewpoint either would appear to be feasible. The vertical pipe alternative would have some advantage in relation to handling sub-assemblies and may also be better as regards pipe routing outside the shield, particularly on the outer panel, where the support leg causes some obstruction.

### 5.3 Roof panels

Many alternative ways in which the shield roof could be subdivided and the cells arranged suggest themselves, but the sketching and draughting effort required to identify clearly a promising method has not been available within the timescale of the present study. The scheme illustrated in Figure 4 is included merely as a notional design. As mentioned earlier in this report, an octagonal vertical section for the shield has been shown here as an alternative to the hexagonal form. It is suggested that these and other embryonic ideas should be discussed with those engaged in the study of remote manipulation of cell sub-assemblies before taking any one scheme much further.

### 5.4 Inner vertical panels

It has been suggested (Ref. 5) that the inner part of the blanket may be of different design from the parts discussed above, since its significance in terms of breeding is lower. In any case, the radial coolant pipe penetrations proposed for the outer panels could not be used here, and therefore the header design would have to be modified considerably. There is no apparent reason why inlet and outlet pipes serving this part of the blanket should not be led vertically through the bottom shield section. If the principle of making all joints outside the shield were retained, this would imply vertically orientated sub-assemblies of full panel height. Although no design work has been done on this part of the blanket, it is considered unlikely that a detailed study would bring to light any difficulties of a fundamentally different nature from those discussed in Section 5 of this report.

### 5.5 Handling of blanket sub-assemblies

In the design concept discussed above, each blanket sub-assembly is supported in the shield from the three fixed points provided by the clamp connections between the shield and the thermal sleeves of the inlet and outlet pipes.

The blanket replacement operation would start with the disconnection and removal of that part of the external pipework which would otherwise obstruct access to the appropriate removeable top section of the shield. Following this, the blanket sub-assemblies suspended from the removeable shield section, shown shaded in Figure 4, would be unclamped from the shield, leaving them suspended in situ by their special lugs on removal of the shield section. After these blanket sub-assemblies have been lifted out, the sub-assemblies in adjacent panels are accessible through the hole, though complicated remotely controlled movements of the manipulating machinery would be necessary, as indicated by the arrows in Figure 4.

The question of connecting the blanket sub-assembly to the manipulator head has not been studied. In the design of sub-assembly proposed the emphasis has been on achieving the nearest approach to homogeneity by close-packing the cells on a triangular lattice, not only within a sub-assembly but between neighbouring sub-assemblies. With such an arrangement the only access to the outlet header (the structural basis of the design) would be through the tricuspid spaces between cells, and the docking features on the manipulator head would therefore be limited to about 40 mm diameter. The feasibility of designing a manipulator head within the severe geometrical constraints would need to be examined. Further study of the problems of the inevitable gaps in a cellular blanket mounted in a quasi-toroidal shield may however suggest that more generous access areas for the manipulator/header connection will in practice be found.

## 6. DISCUSSION

The work reported above provides some illustrations of the engineering problems which would be encountered in the design of a demountable blanket and the surrounding magnet shield of a large lithium cooled Tokamak reactor. Many of the problems are inherent in the broad reactor concept, for example those associated with (a) the toroidal geometry (b) the temperature difference between the various components, and (c) the pressure drops in the lithium circuit due to MHD effects.

The adoption of a polygonal section for the blanket and shield rather than a circular or other curved section reduces the number of variants of blanket sub-assembly geometry, but there would still be a requirement for varying cell diameters on the sloping panels if large streaming gaps at the intersections between sectors were to be avoided. Neither this problem nor the similar one which exists at the vertices of a polygonal sector have been examined.

It is unfortunate that the only well-established suitable material for fabrication of the lithium circuit components, austenitic stainless steel, has a relatively high coefficient of thermal expansion. As has been shown even by the fairly superficial examination of the more obvious differential thermal expansion problems presented here, there are considerable design difficulties in this field. Some of the thermal stress problems would be reduced by the adoption of smaller sub-assemblies consisting of fewer cells, but even with as few as 25 cells per sub-assembly the shield is penetrated by a large number of lithium inlet and outlet pipes, and there must be a strong incentive to maximise the size of sub-assembly in order to keep the cost of the pipework and shield within acceptable bounds. This reinforces the primary reason for designing sub-assemblies of reasonably large size, namely that the outage time for blanket replacement might thereby be kept economically low.

The findings in regard to lithium pressure drop within the transverse magnetic field, and its effect on design pressure of the cells and headers, are fairly encouraging for this type of blanket and pipework arrangement but it is realised that the calculations give only a first approximation to the actual pressures which would be experienced, and more work on this aspect and on external (frictional) pressure drops would be required before confidence could be established in the design. MHD pressure drops might be reduced (Ref. 9 ) by introducing flow dividers in important parts of the pipework which traverse the magnetic field.

Although no study of cost aspects has been included in the present work, it is felt that it would be quite wrong, even at this early stage in the design process, to ignore the fact that both blanket sub-assemblies and shield-structures of the general type discussed would be very expensive.

The cost per unit weight of the blanket sub-assembly would inherently be high because of the complexity of the fabrication and the extremely rigorous quality requirements, and it is perhaps unlikely that significantly more economical design concepts for a lithium-cooled blanket could be found. However, by analogy with fission reactor core and fuel element costs it may be possible to show that a high specific cost of fusion reactor blankets will be tolerable.

It is quite clear that a magnet shield of the general type discussed involves the use of austenitic steel on such a prodigous scale that its viability must be called into question. The possibility of using some cheaper non-magnetic dense material such as hematite to play the main role in regard to gamma attenuation should be considered.

As regards handling of radioactive blanket sub-assemblies during replacement, this study has served merely to stimulate thought, and cannot be regarded as giving any firm indication of the feasibility of such operations. Top access through the shield was chosen, and it appears that this option leads to a reasonably attractive shield design, but it does appear that side access may give more important advantages, connected with the greater amount of space which would be available for manipulative machinery and hot cells around the periphery of the reactor. This merits further study.

In conclusion, it is suggested that the study has given only a very tentative indication that a blanket and shield of the general type specified would be technically feasible. The most serious uncertainties are perhaps connected with the cellular blanket sub-assemblies. Radically different concepts of blanket design, using different module geometry and/or coolant, may be worthy of study to the same depth before further work on the cellular lithium cooled blanket would be justifiable.

## 7. ACKNOWLEDGEMENTS

The author is indebted to Mr. J.T.D. Mitchell of Culham Laboratory for helpful discussion before and during the course of the work reported, and to his colleagues J.R. Stanbridge and B.A. Keen for their constructive criticism and assistance with Appendices A - D.

## 8. REFERENCES

1. STANBRIDGE, J.R. and SHOTTER, H.A. Review of Irradiation Creep and Swelling in a Fusion Reactor Blanket Cell Structure. CLM-R 152, 1975.

2. MITCHELL, J.T.D. and GEORGE, M.W. A Design Concept for a Fusion Reactor Blanket and Magnet Shield Structure. CLM-R 121, 1972.

3. STANBRIDGE, J.R. et al. Design of Stainless Steel Blanket Cells for a Fusion Reactor. CLM-R 127, 1974.

4. CTRD Drawing No. CH 4940/053.

5. MITCHELL, J.T.D. Private communication, 24th September 1974.

6. ASME Boiler and Pressure Vessel Code, Section VIII, 1971.

7. HANCOX, R. and BOOTH, J.A. The use of lithium as coolant in a toroidal fusion reactor, Part II - Stress Limitations. CLM-R 116, 1971.

8. MITCHELL, J.T.D. Private communication, September 1974.

9. HUNT, J.C.R. and HANCOX, R. The Use of Liquid Lithium as Coolant in a Toroidal Fusion Reactor, Part 1 - Calculation of Pumping Power. CLM-R 115, 1971.

# APPENDIX A

## STRESS CALCULATIONS ON SHIELD STRUCTURE

### A.1 LOADING

The individual panels of the shield structure are loaded by their own weight, by atmospheric pressure acting over their outer surface because the inside of the shield structure is evacuated, and by the weight of the blanket assemblies.

The object of this Appendix is to demonstrate that the stresses generated by these loads can be supported by plates of reasonable thickness forming the boundaries of the shield panels. The calculations were carried out early in the contract on a shield thickness of 800 mm as compared to the 600 mm which is now believed to be adequate. The results must therefore be seen in the context of this change, but it is believed that the general conclusions reached are still valid. Furthermore, the calculations take no account of the weight of the blanket structure.

The self-weight loading is based on the distribution of materials shown in Fig. A1.

In calculating the weight/unit length along a shield panel it is assumed that in the mixed section the vertical box sides are included in the 0.8 metal fraction. For the water section the sides have been taken as equivalent to a 0.5 cm thick horizontal layer in the bottom plate. The width of a shield unit is b m.

Then WEIGHT/UNIT LENGTH =

$$\Big\{0.02 \times 7896 + 0.4 \times (0.8 \times 7896 + 0.2 \times 1000) + 0.3 \times 1000 + (0.02 + 0.005) \times 7896 + 0.05 \times 9835\Big\}\, b\ \text{kg/m}$$

$$= \Big\{157.92 + 2606.72 + 300 + 197.4 + 491.75\Big\}\, b$$

$$= \underline{3753.8\ b\ \text{kg/m}}$$

Atmospheric pressure loading is 10335 b kg/m.

### A.2 STRESS CALCULATIONS ON LOWER ELEMENTS OF SHIELD BEAM STRUCTURE

The torus is supported by a single ring of supports positioned below the centre of gravity of the section. The first task then is to calculate the position of the centre of gravity of the section. The system of forces on one sector is shown in Fig. A2 where $V_6$ represents the reaction at the support and $V_1$, $V_2$ are the vertical reactions at A and C respectively due to the upper shield panels. By taking moments about the support G we find the following equation:

$$W_1 x_1 + (V_1 + W_3)\, x_3 = W_2 x_2 + (V_3 + W_4)\, x_4$$

Substituting for the forces, and expressing $x_1$, $x_2$, $x_3$ and $x_4$ in terms of $\overline{x}$ we find $\overline{x} = 2.38$ m.

Now taking moments about E for the beam FE

$$M_{xx} = (V_1 + W_3)\frac{\sqrt{3}}{2}\, l + \frac{\sqrt{3}}{2} \times 3753.8\int_0^l (.61 + .058x)(1 - x)\,dx$$

Evaluating this equation gives the following result for the bending moment at the point x:-

$$M_{xx} = 387591 + 991.5\, l^2 + 31.4\, l^3$$

Similar equations can be derived for the beams EG, and GD. For the part of the beam EG

$$M_{xx} = 422883 + 62570\, l + 1788\, l^2 + 31.4\, l^3 \quad 0 < l < 2.38$$

For the part of the beam GD

$$M_{xx} = 916685 - 116994\, l + 1788\, l^2 + 31.4\, l^3 \quad 2.38 < l < 8.54$$

The bending moments calculated using the above expressions are plotted in Fig. A3. The maximum bending moment, 610 000 kgm, occurs at the point G. It is found that in order to keep stresses within a maximum value of about 140 MN/m$^2$, plate thicknesses of about 50 mm are required in the shield. If the additional weight of the blanket is included these figures should be increased by 22%. The additional weight due to increasing the plate thickness above the 20 mm assumed in the calculation is relatively insignificant but reducing the shield thickness to 600 mm increases the plate thickness requirement to about 60 mm.

In the normal operating condition the shield sector is in equilibirum under gravity and the vertical reaction at the support and no interaction is necessary between neighbouring sectors of the shield. During maintenance in any particular sector, removal of the top shield panels leads to a misalignment of the self-weight of the trough part of the sector and the support reaction, and rotation of this part of the shield is then prevented by forces induced between the sector and its neighbours. By inspection, however, these forces can be seen to be insignificant.

#### Effect of atmospheric pressure

During operation the toroidal space is evacuated and atmospheric pressure acts over the outside surface of the shield structure. The bending moments due to atmospheric pressure have been calculated approximately in order to see what effect they have on the bending moment diagram Fig. A3. In this simplified exercise, symmetry is assumed, i.e. each panel is assumed to be of the same length and width and hence to be considered as an encastre beam.

Then the bending moment at a corner is given by

$$M = \frac{1}{12} p l^2 b$$

and it is found that the bending moment at any section xx is given by

$$M_{xx} = \frac{pb}{2} \left[ - \frac{l^2}{6} + lx - x^2 \right]$$

In evaluating this expression for each panel, a mean value of b has been substituted. This bending moment combined with that due to the deadweight is shown on Fig. A3. It can be seen that the effect of atmospheric pressure is relatively small but it increases the maximum stress at G by about 5%.

A similar exercise on the top panels of the shield structure showed that atmospheric pressure loads are the most important. Because these panels are more lightly loaded than the lower ones however, the plate thickness requirements are less onerous.

## APPENDIX B

## SHIELD COOLING REQUIREMENTS

One of the 96 sectors of the shield is considered here. It is taken to be of hexagonal form, the six panels being designated A-F as in Fig. B1. The material composition of each panel is taken to be as shown in Fig. A1 (Appendix A).

The volumetric heat generation rate appropriate to the chosen wall loading of 1.31 MW/m$^2$ has been derived from a Culham estimate of energy absorption in a shield with the same thickness and material distribution, but for a reactor with a wall loading of 10 MW/m$^2$. This estimate, shown in fig. B2, when scaled down in the ratio 1.31:10, gives the following mean volumetric heating rates in the various layers of the shield:

| Material of layer | Mean heating rate(W/m$^3$) |
|---|---|
| 0.8ss,0.2 borated $H_2O$ | 19650 |
| borated $H_2O$ | 272 |
| lead | 10.5 |

The volumes of the different layers of material in each panel and the corresponding rates of heat generation are shown in Table B1.

The coolant water flow rate required per shield sector, assuming a temperature rise of 30°C, is 2.66 litres per second, divided appropriately between the panels.

The total heat to be removed from the 96 sectors of the shield is 32 MW, calling for a cooling water flow rate of about 250 l/s.

| | Panel | | | |
|---|---|---|---|---|
| | A,E(each) | B,D(each | C | D |
| Volumes ($m^3$) | | | | |
| 0.8ss,0.2 $H_2O$ | 3.46 | 2.19 | 1.56 | 4.00 |
| $H_2O$ | 2.30 | 1.46 | 1.04 | 2.67 |
| Pb | 0.576 | 0.365 | 0.260 | 0.667 |
| Heat generation rates (W) | | | | |
| 0.8ss,0.2 $H_2O$ | 67989 | 43034 | 30654 | 78600 |
| $H_2O$ | 626 | 397 | 283 | 726 |
| Pb | 6 | 4 | 3 | 7 |
| Total per panel | 68621 | 43435 | 30940 | 79333 |

Table B1. Material volumes and heat generation rates in shield panels

## APPENDIX C

## PROBLEMS ARISING FROM HEAT CONDUCTION AND RADIATION WITHIN THE BLANKET SUB-ASSEMBLY AND SHIELD

There are two problems which will be discussed under this heading: first the problem of heat dissipation from the structural member in a design concept in which a group of cells are mounted on separate frame, see Section 4.1 (a); secondly, the more general problem of heat losses between the blanket/shield assembly and the consequent requirements for thermal insulation will be discussed.

### C.1 HEAT DISSIPATION FROM INDEPENDENT FRAME MEMBER

There are two main unknowns about which assumptions must be made;

- heat generation rate,
- dimensions of the structure.

The heat generation rate is obtained from a graph of energy absorbed against distance into the shield obtained from Culham Laboratory (Fig. B2). The structural member must be situated at a position between the back of the blanket and the front of the shield, and this is taken to correspond to the position $x = 0$ on the graph. Then the energy absorbed (assumed constant through the thickness of the member) = 0.8 W/cm$^3$.

A framework fabricated from 6 in x 5 in I-beams, i.e. having webs approximately 15 cm deep and 12.5 cm flanges, would appear to offer adequate stiffness and dead-load bearing capability, and for the present purposes a 1 m length of such a beam is considered. With a standard section beam the heat generation rate is 4345 W/m. All this internally generated heat is assumed to be dissipated by radiation from the outer flange to the front wall of the shield. It is further assumed that no heat enters the structure from the blanket cells or pipework. Then with a view factor of unity and an emissivity at each surface of 0.6, the following radiation heat transfer relation can be written down

$$\frac{4345}{0.125} = 5.69 \times 0.43 \left\{ \left[\frac{T_h}{100}\right]^4 - \left[\frac{353}{100}\right]^4 \right\}$$

from which $T_h = 1094\text{K} = 821^\circ\text{C}$

i.e. in order to radiate all the heat generated within the beam to the shield, its outer temperature must be at a temperature 821°C.

There is also a temperature gradient $\Delta T$ across the beam. If for simplicity it is assumed that the heat is generated uniformly in an equivalent rectangular section we find $\Delta T = 552^\circ\text{C}$ i.e. the temperature at the inside surface of the structure $= 552 + 821 = 1\,373^\circ\text{C}$.

This temperature is indicative only, it being dependent, as stated above, on the heat generation rate and the beam dimensions. Some heat would also be lost to the inlet header and also from the sides of the beam to the shield depending on the geometry of the blanket cell unit and the proportion of the beam sides "visible" from the shield. These considerations will not reduce the main force of the argument demonstrated by the calculations which indicate that a design concept using an independent frame would involve serious problems associated with the requirement to remove heat from the frame and compatibility problems arising from differential thermal expansion.

## C.2 HEAT LOSS FROM BLANKET SUB-ASSEMBLY TO SHIELD

The potential mechanisms for heat loss from the blanket sub-assembly to the shield can best be understood by examining the layout of the proposed arrangement, shown on Fig. 3. The mechanisms are:

- radiation from back side of outlet header to shield,
- radiation across the thermal sleeve,
- conduction of heat along the length of thermal sleeve.

Each of these mechanisms will be considered in turn, starting with radiation from the outlet header.

### Radiation from outlet header to shield face

Some heat will also be radiated from the inlet header but this will be small in comparison to that from the outlet header and, for the moment, will be neglected. Although the inlet headers obscure some of the radiating area of the outlet headers, it will be assumed for simplicity that the outlet headers can radiate heat to the shield over the whole of their area.

Then, for an outlet header surface temperature of 500°C, a shield surface temperature of 80°C, and assuming emissivities at the two surfaces of 0.6 we find the heat radiated per unit area is given by

$$q = 5.69 \times 0.43 \left\{ \left[\frac{773}{100}\right]^4 - \left[\frac{353}{100}\right]^4 \right\}$$

$$= 8350 \text{ watts/m}^2$$

The total area of the inside surface of the shield is obtained approximately by assuming true toroidal geometry, and is given by

$$A = 4\pi^2 rR$$
$$= 4\pi^2 \times (5.79 + 1.3) \times 16.73$$
$$\sim 5\,000 \text{ m}^2$$

Then the total heat lost by radiation from the outlet header surface is about 42 MW.

The consequences of such a loss of useful heat are a loss of revenue to the station equal to the value of 42 MW of heat over a period of, say, 20 years, and an increase in the cost of the shield cooling plant. The heat loss could be reduced by putting thermal insulation on the outlet duct surface and it would be worthwhile to do so if the cost of the insulation was less than the present worth cost of the lost heat (the increased cost of the shield cooling will be neglected). Very simple calculations can be used to show that thermal insulation is worthwhile. One form of insulation which would be suitable in this application is stainless steel foil and mesh, e.g. successive layers of 0.004 inch foil and 0.036 inch wire mesh. A rough figure for the cost of this insulation is £8.6 per m² per layer (erected), and it will be shown below that approximately 15 layers will be required. It is believed that such a pack could be fitted without increasing the overall dimensions of the reactor. With these figures the total cost of the insulation is about £650 000 and it is estimated that it is economically worthwhile to reduce the heat loss to about 3 MW, i.e. by about an order of magnitude on the estimated loss.

In order to achieve this it can be shown that the outer surface of the insulation should have a temperature no greater than about 175°C. It should be noted that this has the incidental advantage of eliminating heat losses between the outlet and inlet coolant over this area. The remaining question to be answered is how many layers of thermal insulation are required to achieve a temperature reduction from 500°C to 175°C. The performance of the proposed type of insulation is assisted by the vacuum environment in which the only forms of heat transfer are radiation plus a small amount of conduction across the contact points between the foil and mesh. Based on the assumption of radiation only it can be shown that a thickness consisting of 10 layers is adequate but if some allowance is made for the additional conduction then it may be necessary to increase the thickness to about 15 layers, having a total thickness of about 18 mm.

### Heat losses across the thermal sleeve

Heat is lost from the outlet thermal sleeve to the shield by radiation across the gap between the sleeve and shield and by conduction down the sleeve, which is shown in Fig. 3. The effect of the radiation heat transfer across the gap is to create a non-linear temperature gradient down the thermal sleeve which will lead to thermal stresses. A fairly simple two-dimension network could be used to determine the temperature distribution in the thermal sleeve, but this and the subsequent calculation of thermal stress is outside the scope of this work.

A fairly crude assessment of the heat loss to the shield can be made by assuming that all the radiation heat loss is in the radial direction and that the thermal sleeve has a uniform temperature. Then applying the Stefan-Boltzman equation using these assumptions the radial heat flow is 4178 W/m$^2$ and the sleeve temperature is 384°C. Taking notional dimensions from Fig. 3 it can then be shown that the heat loss per blanket cell unit is 2624 W by radiation, compared with only 89 W by axial conduction (this latter calculated assuming a linear temperature gradient). For the whole reactor, if there are 85 500 cells with 25 cells in each unit, the total heat loss by this mechanism to the shield is 9 MW. Since nearly all of this is due to radiation it could be reduced by insulating the thermal sleeve, though it may not be economically worthwhile to do so. It is suggested that the case for thermal insulation should be considered when a detailed assessment of thermal stresses is undertaken.

### Radiation heat loss between the outlet header and inlet header

It can be seen from Section xx of Fig. 3 that the inlet feeder pipe to each cell passes through the flat outlet header which contains lithium at a temperature of 500°C. The inlet feeder passes through a clearance hole and it is assumed here that the clearance is sufficiently large to accommodate the differential thermal expansion between the inlet and outlet headers without mechanical interference. In this case the heat transferred is not lost from the system and the only consequence is a drop in the outlet lithium temperature which leads to a small loss of thermal efficiency of the reactor.

Applying the Stefan-Boltzmann relationship it is found that the heat lost per cell is 96.7 W. It is estimated that the thermal output per cell is 58.4 kW, so the heat lost represents 0.16%, or, about 0.35°C on the lithium outlet temperature. This applies to the relatively small area where the inlet header passes through the outlet header. Within the cell itself there is also a heat interchange between the inlet and outlet flows but for present purposes this is regarded as part of the internal cell performance and it is assumed that the cell is designed to give a specified temperature at its outlet. This specified temperature may be determined by cell wall structural considerations.

## APPENDIX D

## DESIGN PRESSURE FOR OUTLET HEADER

The design pressure for the outlet header must allow for:

(a) Pressure drop through header
(b) Pressure drop in outlet pipework
    (i) through shield
    (ii) between shield and magnet coil
    (iii) through magnet coil zone
    (iv) from outside magnet coil to pump inlet
(c) Static pressure at pump inlet.

### Pressure drop through header

If, as suggested in Section 4.3.4 of the report, the header is arranged with its length parallel to the direction of the magnetic flux, the MHD pressure drop in the header will be negligible. Furthermore the friction pressure drop will be small compared with that in the external part of the circuit. Thus pressure drop through the header will be ignored for the present purposes.

### Pressure drop in outlet pipework

MHD effects predominate in (b) (i) (ii) and (iii) above.

The following equation, derived from Ref. 7, is used to evaluate these components of pressure drop:

$$\Delta_p = \frac{W}{\rho A}\,\sigma_w\,\frac{t}{a}\int B^2\,dl$$

where $\Delta p$ = pressure drop in a length of pipe l
$W$ = mass flow of lithium in pipe
$\rho$ = density of lithium
$A$ = cross-sectional area of flow
$\sigma_w$ = electrical conductivity of pipe wall
$t$ = pipe wall thickness
$a$ = pipe internal radius
$B$ = transverse magnetic flux
$dl$ = element of pipe length

It will be assumed that the outlet pipe has a diameter of 215 mm and a wall thickness of 1.5 mm from the header outlet to the outer surface of the shield, and a diameter and wall thickness of 300 mm and 2.1 mm respectively downstream of this point. Each outlet pipe serves a 25-cell sub-assembly requiring a mass flow of 25 x 0.081 = 2.025 kg/s; $\rho$ = 516 kg/m$^3$; and $\sigma_w$ = 0.917 x 10$^6$ ohm$^{-1}$ m$^{-1}$ at 500°C.

The variation of magnetic flux with distance from the reactor axis is given in Fig. D1. It rises linearly from zero to 8 tesla through the thickness of the inner limb of the magnet coil, is inversely proportional to distance from the reactor axis through the zone within the coil, and then decreases linearly to zero through the thickness of the outer limb of the coil (Ref. 8).

From Fig. D1 it can be seen that for most sub-assemblies the largest component of pressure drop will be in the rather long flow paths between the shield and the outside of the magnet coil zone. The optimal arrangement of pipwork from this viewpoint would be one in which pipes were routed outwards from sub-assemblies at radii greater than $R_{crit}$, and inwards from sub-assemblies at radii smaller that $R_{crit}$, where $R_{crit}$ is such that

$$\int_{R_2}^{R_{crit}} B^2\,dR + \int_{R_1}^{R_2} B^2\,dR = \int_{R_{crit}}^{R_3} B^2\,dR + \int_{R_3}^{R_4} B^2\,dR$$

For the reactor parameters being considered, $R_{crit} \simeq 13$ m, and the maximum pressure drop between the outer surface of the shield and the outside of the magnet coil zone is 0.137 MN/m$^2$.

To this must be added the pressure drop through the shield at the critical radius. Allowing for a path length of 1 m, this component is 0.047 MN/m$^2$.

Thus the maximum total MHD pressure drop in the outlet pipe is 0.137 + 0.047 = 0.184 MN/m$^2$.

### Pressure drop from outside magnet coil to pump inlet

In Ref. 3 it is deduced that a reasonable design aim in regard to pressure drop in the parts of the circuit external to the magnet coils (item (c) above) would be 0.083 $P_w$ where $P_w$ is the wall loading. In the present case $P_w$ = 1.31 MW/m$^2$ and the corresponding external circuit pressure drop is therefore 0.11 MN/m$^2$.

### Static pressure at pump inlet

We adopt the assumption in Ref. 3 that the absolute pressure at lithium pump inlet (item (b) (iv) above) should be 0.2 MN/m$^2$.

### Total pressure in outlet header

Summing the above components of pressure drop and adding them to the pump inlet pressure results in an absolute pressure of 0.494 MN/m$^2$ in the header.

## APPENDIX E

## THERMAL STRESSES WITHIN THE BLANKET STRUCTURE AND SUPPORT

### E.1 CELL INLET PIPES

In order to assess the capability of the re-entrant cell inlet pipe arrangement of accommodating differential thermal expansions within the sub-assembly, the case of the inlet pipe most remote from the mid-point of the inlet header is considered below.

All components other than the concentric lengths of pipe passing through the outlet header and cell are regarded as infinitely stiff; thus the system is treated as two parallel cantilevers rigidly coupled to each other at one end and direction-fixed but with relative lateral displacement at the other end. Figure E1 shows this system, and gives the nomenclature and sign convention adopted for the following analysis.

From simple bending theory, the equations for the inner tube are:

$$EI_1 \frac{d^2y}{dx^2} = M_1 - Fx$$

$$EI_1 \frac{dy}{dx} = M_1 x - F\frac{x^2}{2} + A \qquad (1)$$

$$EI_1\, y = M_1 \frac{x^2}{2} - F\frac{x^3}{6} + Ax + B \qquad (2)$$

$A = B = 0$ since $\frac{dy}{dx} = y = 0$ when $x = 0$

Similarly for the outer tube:

$$EI_2 \frac{dy}{dx} = M_2 x - F\frac{x^2}{2} \qquad (3)$$

$$EI_2\, y = M_2 \frac{x^2}{2} - F\frac{x^3}{6} \qquad (4)$$

At joined end slopes are equal and opposite, hence:

$$(1) \text{ and } (3) \rightarrow \frac{1}{I_1}\left[M_1 l_1 - F\frac{l_1^2}{2}\right]$$

$$= -\frac{1}{I_2}\left[M_2 l_2 - F\frac{l_2^2}{2}\right] \qquad (5)$$

At other end of outer tube:

$$\Delta = \frac{1}{EI_1}\left[M_1\frac{l_1^2}{2} - F\frac{l_1^3}{6}\right]$$

$$+ \frac{1}{EI_2}\left[M_2\frac{l_2^2}{2} - F\frac{l_2^3}{6}\right] \qquad (6)$$

For equilibrium of system:

$$M_1 - M_2 = F(l_1 - l_2) \qquad (7)$$

Taking the following values: $l_1$ = 750 mm,
$l_2$ = 670 mm,

mean inner tube radius

$\bar{r}_1$ = 31 mm, wall thickness $t_1$ = 2 mm, →
$I_1 = 1.872 \times 10^5$ mm$^4$,

mean outer tube radius

$\bar{r}_2$ = 38 mm, wall thickness $t_2$ = 2 mm, →
$I_2 = 3.447 \times 10^5$ mm$^4$,

E = 0.207 MN mm$^{-2}$,

and solving equations (5), (6) and (7) for F, $M_1$ and $M_2$ in terms of the relative displacement Δ mm gives:

$$\underline{F = 791\ \Delta \text{N}}$$

$$\underline{M_1 = 307\ \Delta \text{Nm}}$$

$$\underline{M_2 = 243\ \Delta \text{Nm}}$$

The maximum thermally induced bending stress occurs at the outer (direction-fixed) end of the inner tube and is given by

$$\hat{\sigma}_{th} = \pm \frac{M_1 \hat{r}_1}{I_1}$$

$$= \pm \frac{307\Delta \times 10^3 \times 32}{1.872 \times 10^5}$$

$$= \pm \underline{52.5\ \Delta\ \mathrm{N\,mm^{-2}}}$$

In calculating $\Delta$ it is now assumed that the inlet and outlet headers are only connected via the low-stiffness connections formed by the cell inlet pipes, and therefore that neither header is constrained by the other against thermal movements. This implies that the inlet header will expand relative to the shield as from a point mid-way between the centre-lines of the twin inlet pipes if this arrangement is used, or as from the centre-line of a single inlet pipe (see Section E2 below).

Taking the operating temperatures of the shield, inlet and outlet headers as 60°C, 300°C and 500°C respectively, and the thermal coefficient of expansion for stainless steel as $18 \times 10^{-6}\ {}^{\circ}\mathrm{C}^{-1}$, a displacement vector diagram for the centre-line of the end cell and its inlet pipe gives the lateral displacement for this cell.

$$\underline{\Delta = 4.86\,\mathrm{mm}},$$

which, using the expression derived above, gives a maximum thermal stress

$$\underline{\hat{\sigma}_{th} = \pm 255\ \mathrm{N\,mm^{-2}}}$$

It should be noted that this thermal stress is proportional to tube diameter but independent of wall thickness. It is a secondary stress as defined in Section III of the ASME Boiler and Pressure Vessel Code. The primary membrane stresses due to lithium pressure are relatively low. For example, with a tube wall thickness of 1 mm (which is perhaps more likely than the 2 mm thickness assumed above), and a lithium pressure of 1 $\mathrm{N\,mm^{-2}}$ (which is well above the expected value), the hoop stress is 31 $\mathrm{N\,mm^{-2}}$ and the longitudinal membrane stress is 15.5 $\mathrm{N\,mm^{-2}}$. The stress system is two-dimensional, and the "maximum stress intensity" as defined in the ASME Code is 255 + 15 = 270 $\mathrm{N\,mm^{-2}}$. For a typical austenitic steel at 300°C the Code specifies an "allowable stress" of 16 300 $\mathrm{lb\,in^{-2}}$ or 112 $\mathrm{N\,mm^{-2}}$, and for the relevant case of combined primary and secondary stress, a maximum stress intensity of 3 times this, or 336 $\mathrm{N\,mm^{-2}}$ is allowed.

Thus the proposed type of design appears to be capable of accommodating thermal movements without overstressing the material of the cell inlet pipes. The above analysis is indicative only; for example the effect of the pipe bend at entry to the cell has been ignored. However, if a more detailed analysis showed stresses to be rather too high the inlet pipe diameter could be reduced somewhat, thus reducing the thermal stress in proportion. Bearing in mind the short lithium flow path along the tube, this could be done without a serious increase in pressure drop.

## E.2 SUB-ASSEMBLY INLET DUCTS

Using simple bending theory, the thermally-induced bending stress in the thermal sleeves of a pair of inlet pipes arranged as in Figs. 3 and E2 has a maximum value of

$$\frac{3\,E\,a\,d\,\alpha\Delta T}{2\,l^2}$$

where $E$ = Young's Modulus
$a$ = distance between inlet pipes
$d$ = diameter of thermal sleeves
$\alpha$ = coefficient of thermal expansion
$\Delta T$ = temperature difference between shield and inlet header
$l$ = length of thermal sleeves

This pessimistically ignores flexibility in all components except the thermal sleeves, but gives a close enough approximation for the present purpose. Using the appropriate dimensions for the design illustrated in Fig. 3, a thermal bending stress of about 500 $\mathrm{N\,mm^{-2}}$ is obtained. This is unacceptably high, and indicates that further design work would be necessary on this feature. Possible changes to improve the situation might include:

(a) The use of re-entrant sleeves, i.e. concentric sleeves attached to each other at their inner ends, and to the inlet pipe and shield respectively at their outer ends. The stiffness of the assembly could thereby be approximately halved, with a corresponding reduction in thermal bending stress;

or

(b) Separation of the inlet header into two distinct sub-headers.

## APPENDIX F

## STRESSES IN THERMAL SLEEVES DUE TO DEAD LOAD

The weight of a sub-assembly such as the one shown in Fig. 3 is approximately 1.5 t including the lithium, and the centroid lies about 1.25 m inside the outer surface of the shield where the sleeves are clamped.

In the case of a sub-assembly near the equatorial plane of the toroid the sleeves are subjected to bending due to the overhung dead load.

In order to assess the stresses and deflections due to this load the following dimensions are assumed:

| | | | |
|---|---|---|---|
| Outlet sleeve | mean diameter | 250 | mm |
| " " | thickness | 10 | mm |
| Inlet sleeve | mean diameter | 185 | mm |
| " " | thickness | 7.5 | mm |

All three sleeves are pessimistically taken to act as cantilevers 1.25 m long, i.e. as if they extended to the centroid of the sub-assembly, and the dead load is shared in the ratio of their flexural rigidities, i.e. the outlet sleeve takes

$$1.5 \times \frac{250^4}{250^4 + 2 \times 185^4} = 0.94\ \text{t}$$

and each inlet sleeve takes 0.33 t.

Then the maximum bending stress, which occurs at the outer end of the outlet sleeve, is given by

$$\sigma_{max} = \frac{M\,y_{max}}{I}$$

$$= \frac{0.94 \times 9810 \times 1250 \times 130}{\pi \times 125^3 \times 10} = 24.3\ \text{N/mm}^2$$

The end deflection of the outlet sleeve would be given by

$$\delta = \frac{Wl^3}{3EI} = \frac{0.94 \times 9810 \times 1250^3}{3 \times 0.2 \times 10^6 \times \pi \times 125^3 \times 10}$$

$$= \underline{0.49\ \text{mm}}$$

The above rough assessment indicates that a support system of the type proposed would not be likely to present strength or rigidity problems.

---

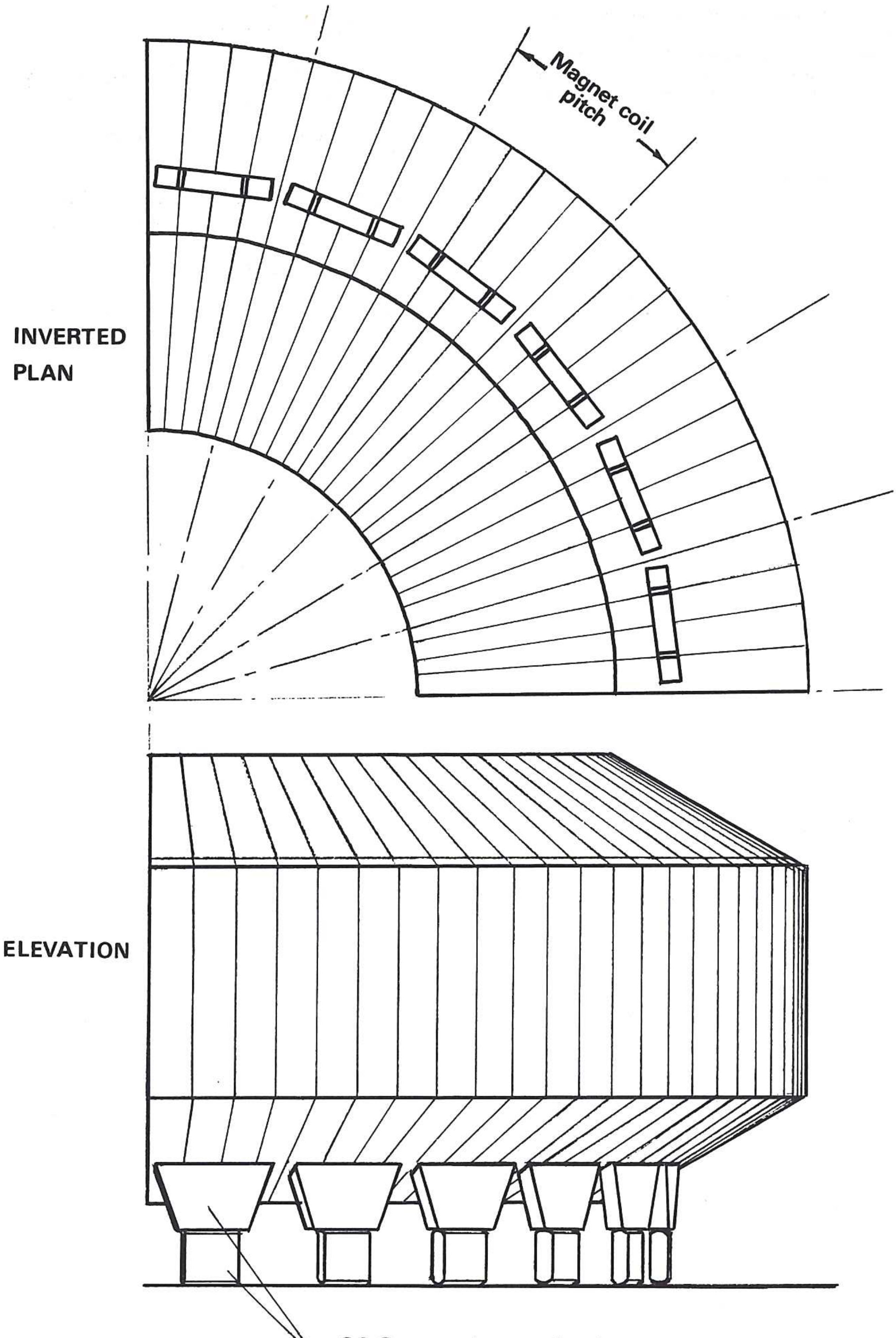
Magnet coil pitch
INVERTED PLAN
ELEVATION
24 Support legs and rollers

Fig.1 General arrangement of shield

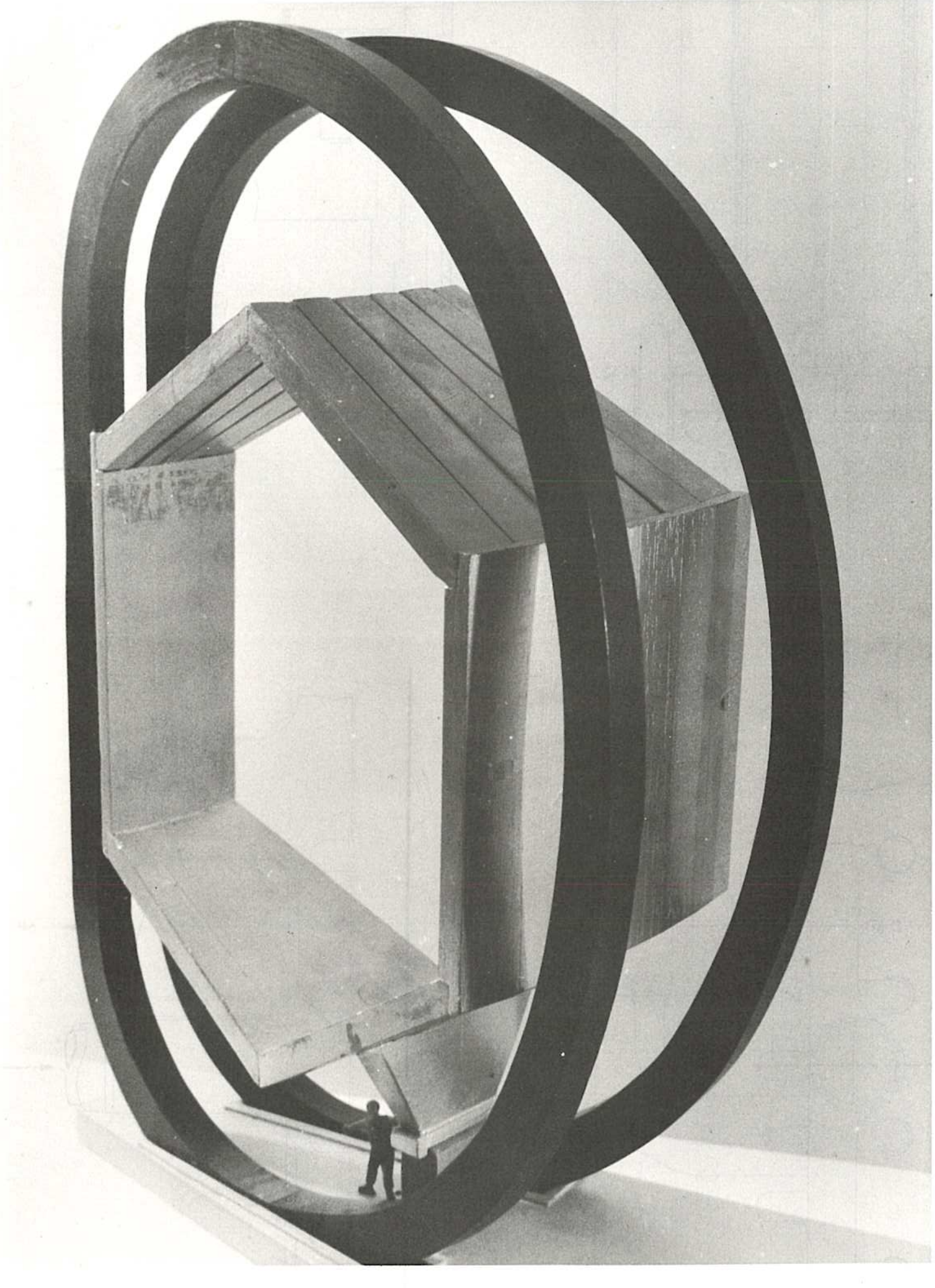

Fig.2 Model of part of shield with adjacent magnet coils

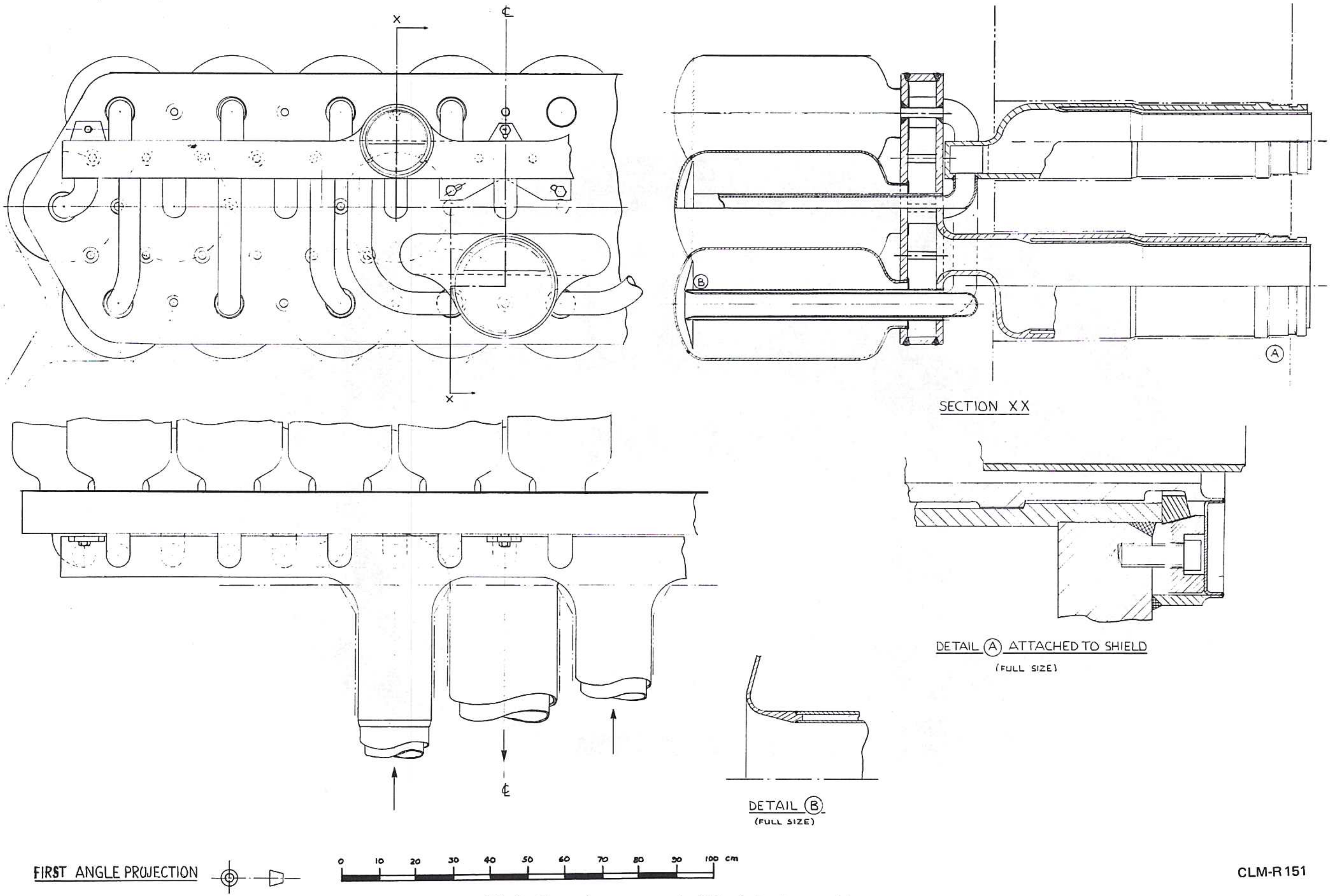
X
℄
X
SECTION XX
Ⓐ
Ⓑ
DETAIL Ⓐ ATTACHED TO SHIELD
(FULL SIZE)
℄
DETAIL Ⓑ
(FULL SIZE)
FIRST ANGLE PROJECTION
0
10
20
30
40
50
60
70
80
90
100 cm

Fig.3 General arrangement of blanket sub-assembly

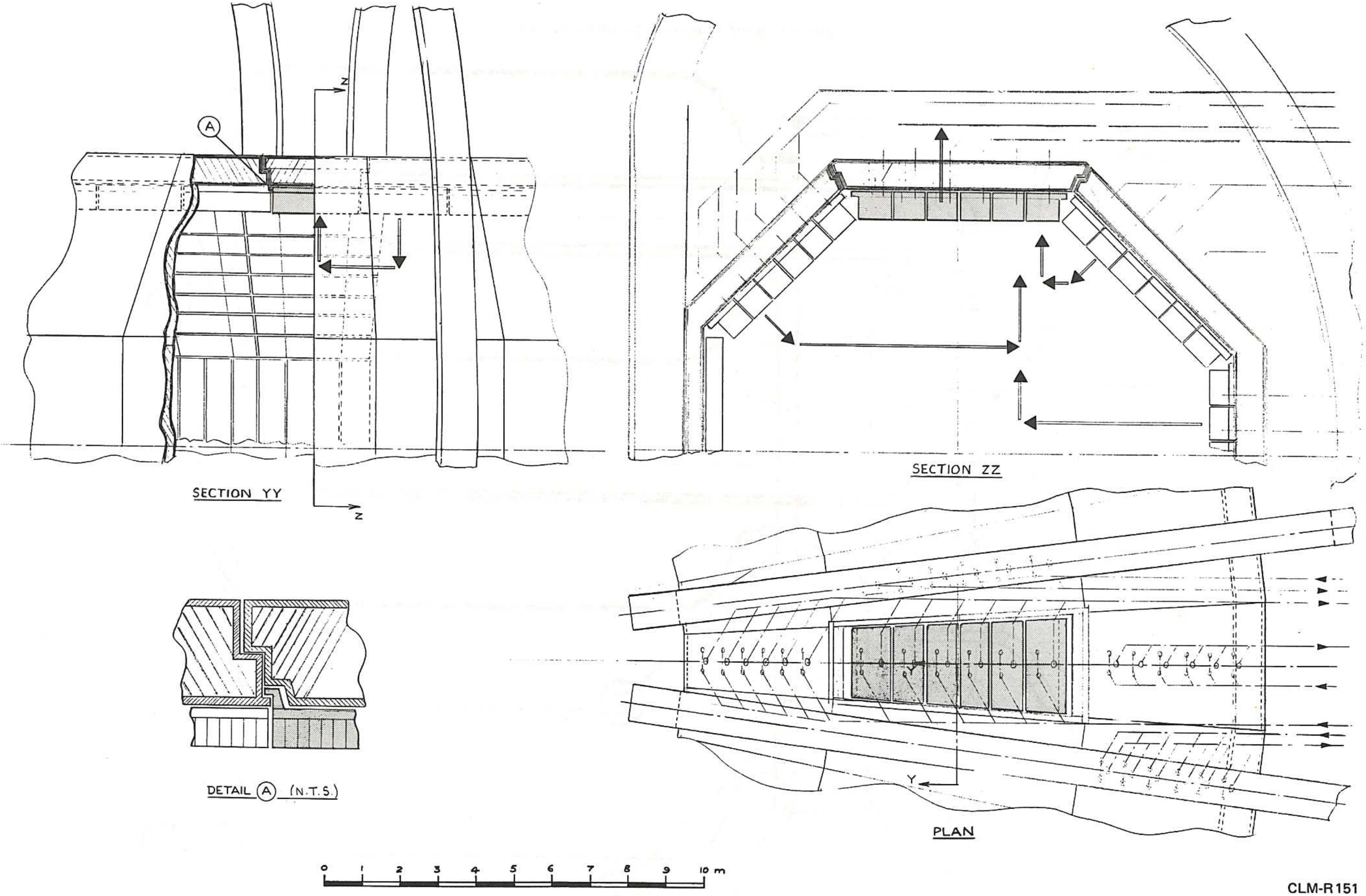
A
N
N
SECTION YY
SECTION ZZ
DETAIL A (N.T.S.)
Y
Y
PLAN
0
1
2
3
4
5
6
7
8
9
10 m

Fig.4 Notional scheme for access to blanket and handling of sub-assemblies

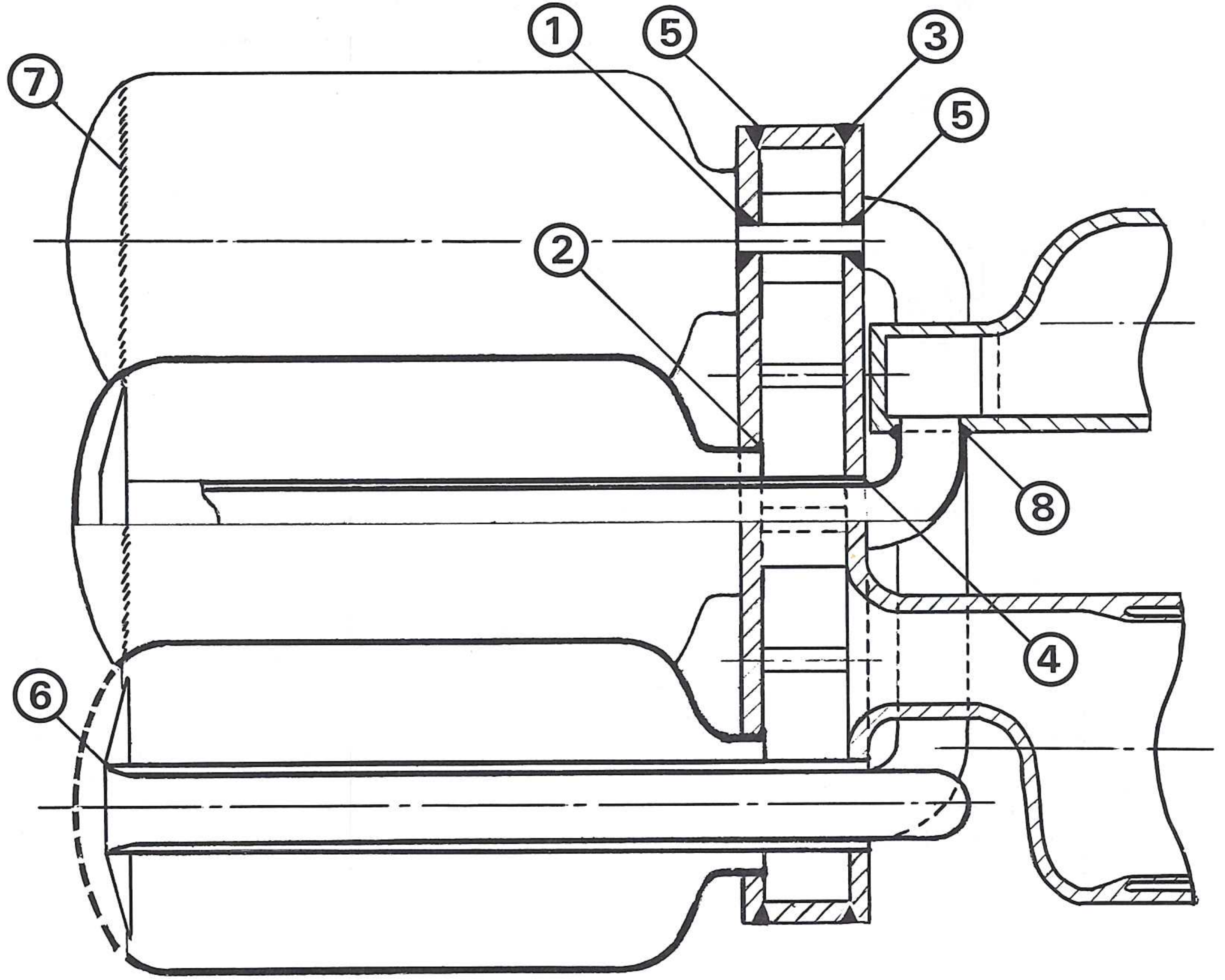

Fig.5 Sequence of operations during assembly

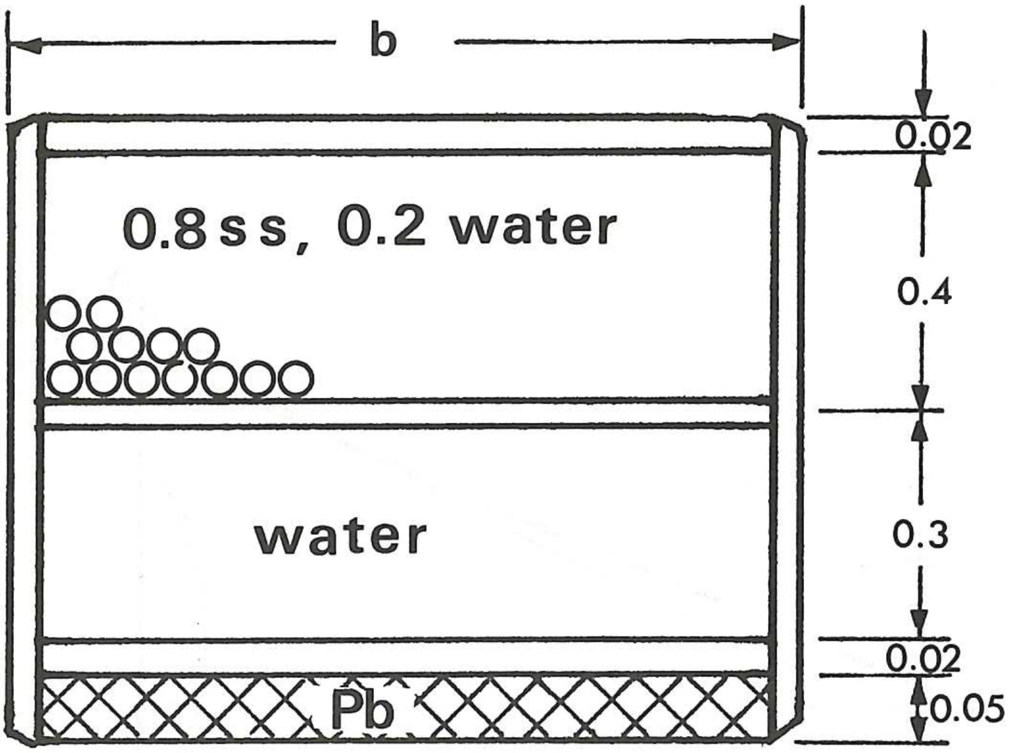
b
0.8 s s, 0.2 water
water
Pb
0.02
0.4
0.3
0.02
0.05

Fig.A.1 Material composition of shield

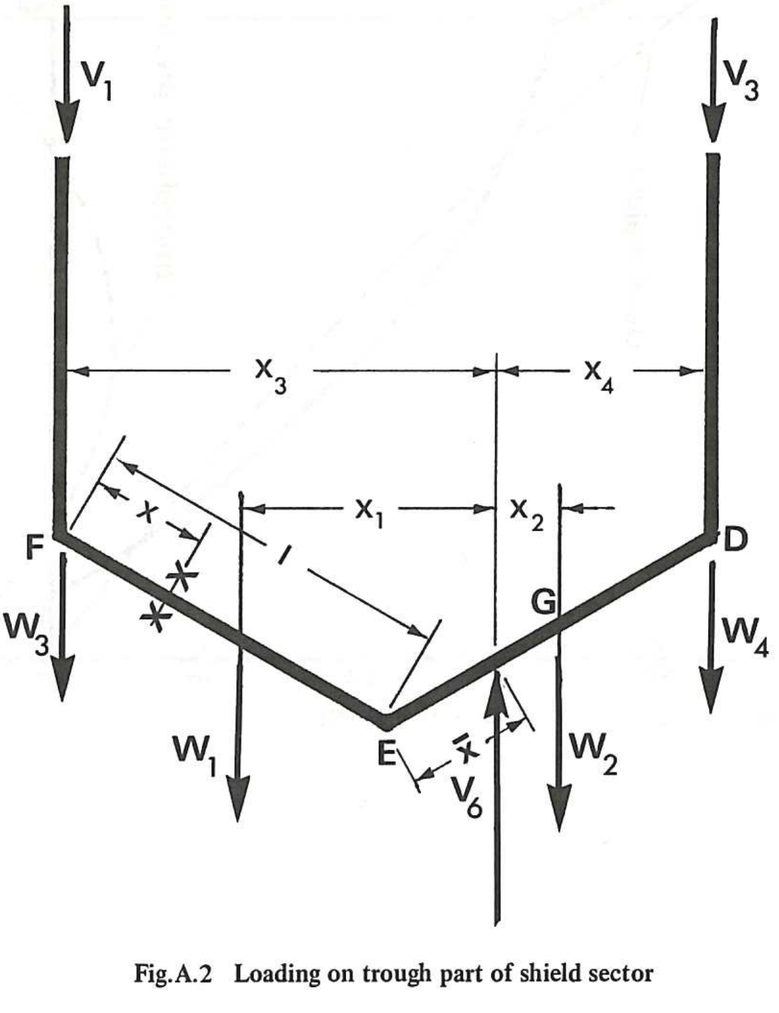
V1
V3
x3
x4
x
x1
x2
l
F
D
G
W3
W4
W1
E
x̄
V6
W2

Fig.A.2 Loading on trough part of shield sector

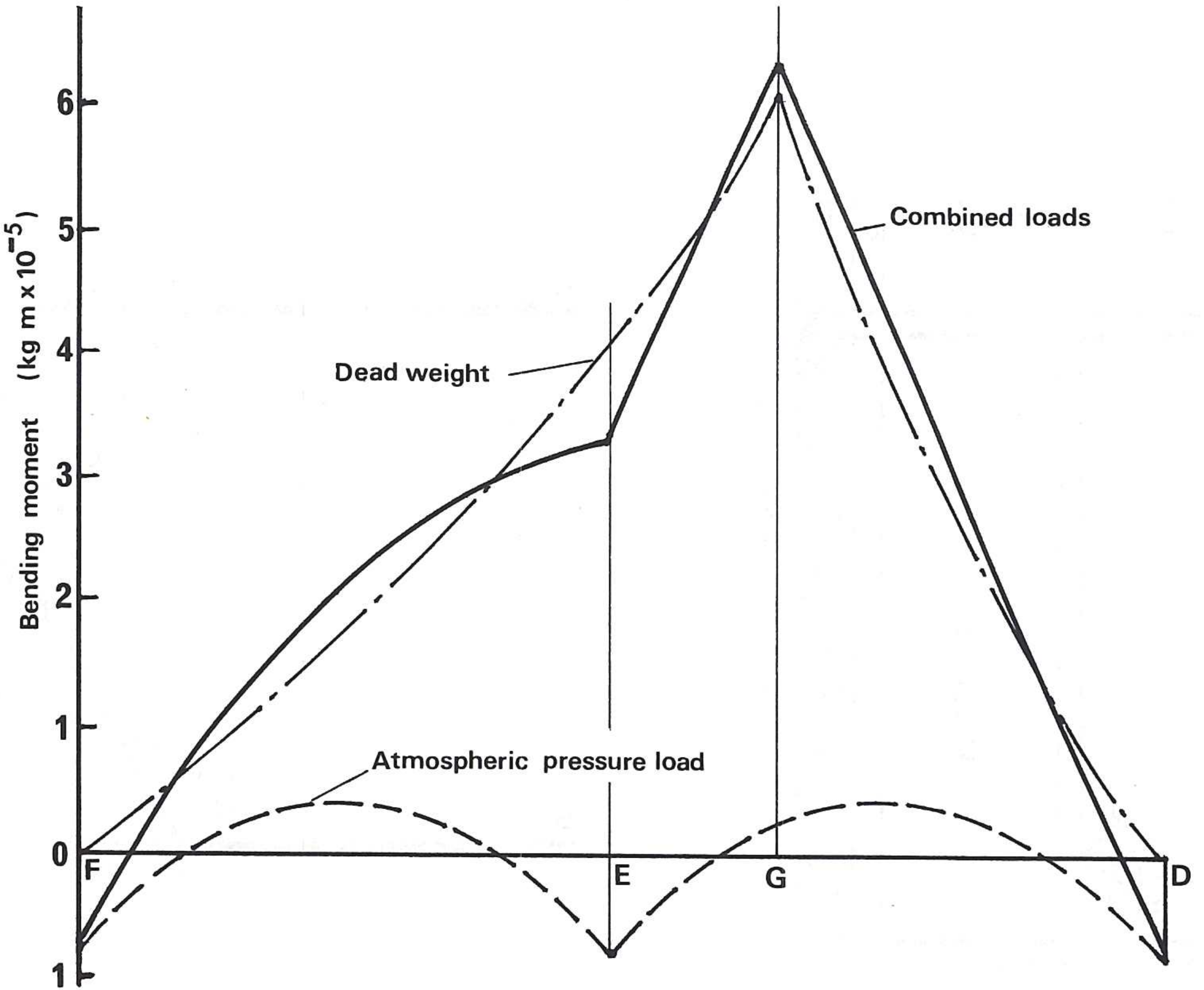

Fig. A.3 Bending moments on shield sector

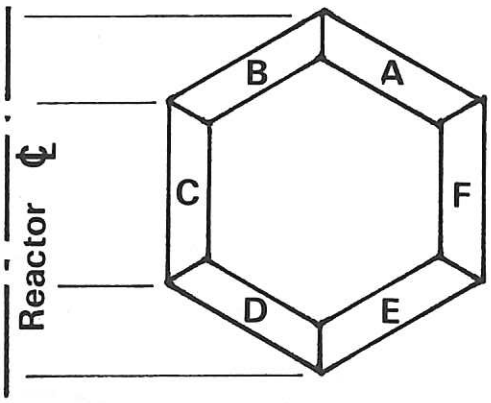
Reactor ℄
A
B
C
D
E
F

Fig.B.1 Key to shield sector panels

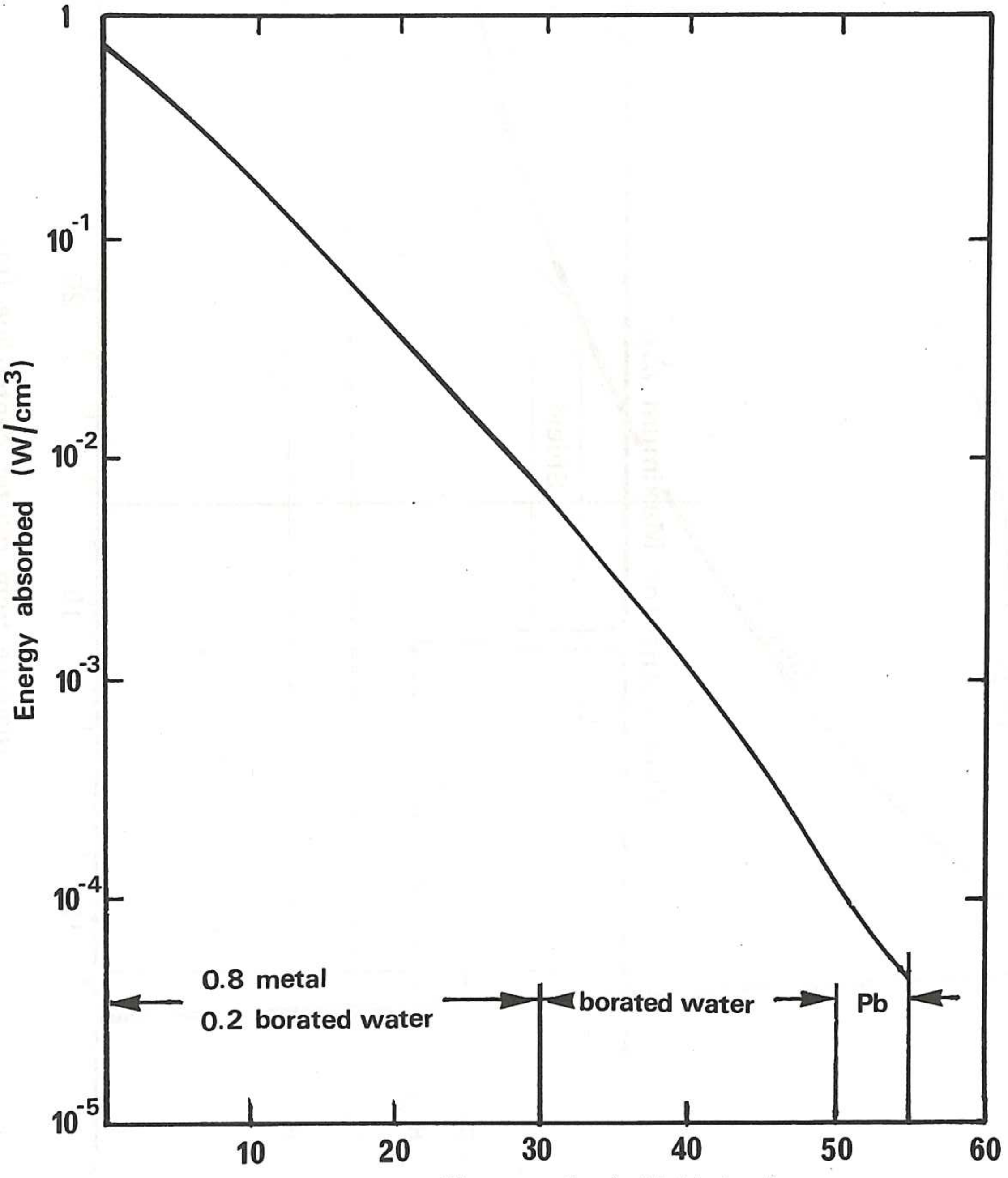

Fig.B.2 Energy absorption in shield

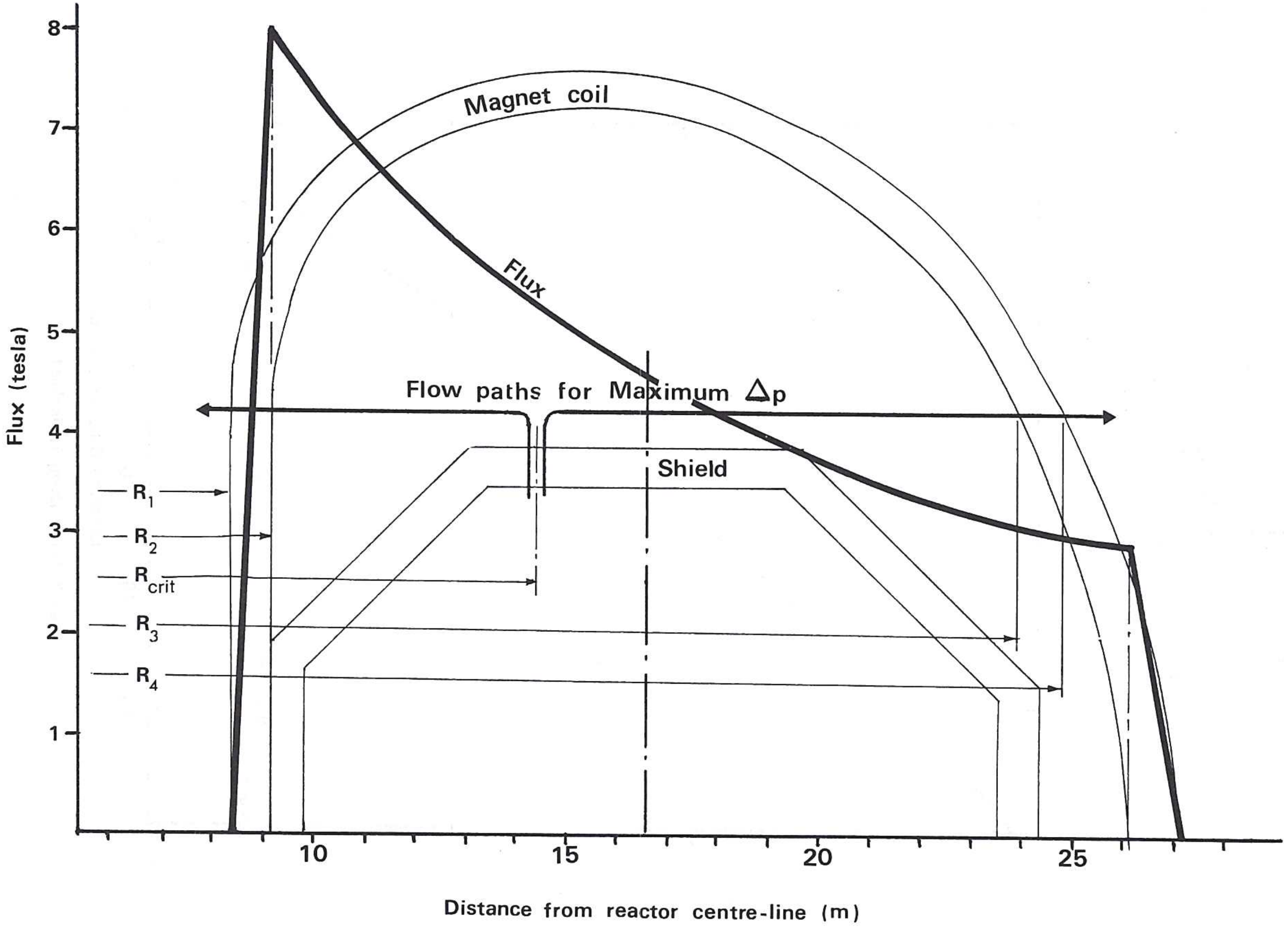

Fig.D.1 Magnetic flux variation and lithium flow paths

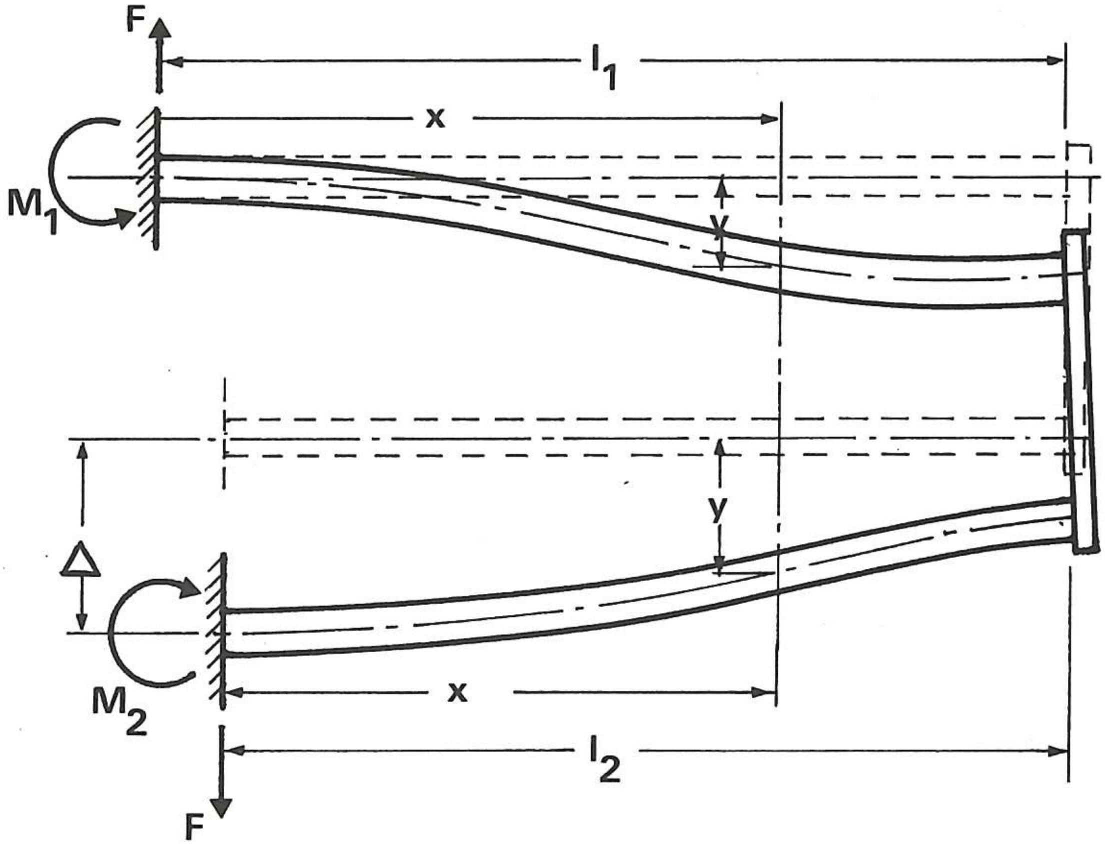
F
l1
x
M1
y
Δ
y
M2
x
l2
F

Fig.E.1 Idealised cell inlet pipe system

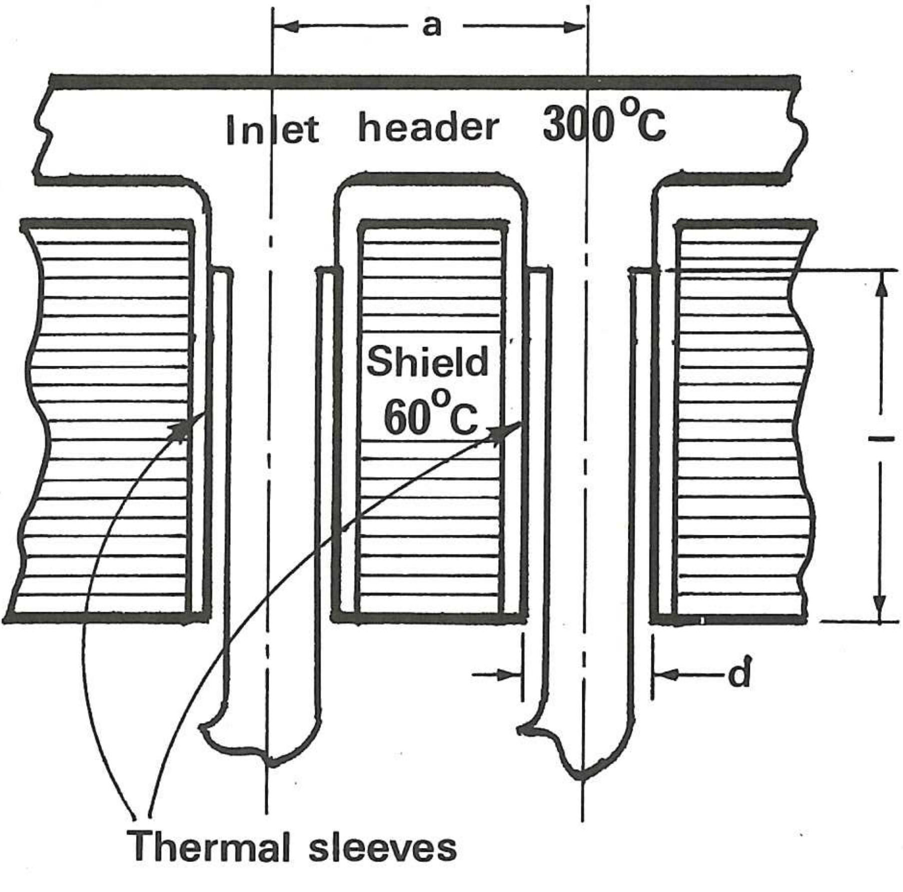
a
Inlet header 300°C
Shield
60°C
l
d
Thermal sleeves

Fig.E.2 Schematic arrangement of inlet thermal sleeves

HER MAJESTY'S STATIONERY OFFICE

*Government Bookshops*

49 High Holborn, London WC1V 6HB
13a Castle Street, Edinburgh EH2 3AR
41 The Hayes, Cardiff CF1 1JW
Brazennose Street, Manchester M60 8AS
Wine Street, Bristol BS1 2BQ
258 Broad Street, Birmingham B1 2HE
80 Chichester Street, Belfast BT1 4JY

*Government publications are also available*
*through booksellers*